International Journal of Scientific Research & Engineering Trends
Volume 8, Issue 2, Mar-Apr-2022, ISSN (Online): 2395-566X

Performance and Modeling for the Home Solar Thermal and Power Supply System and Energy Management

M. Tech. Scholar Rajkumar Baghele, Asst Prof. Shyam Kumar Barode, HOD Sachin Jain
Department of Mechanical Engineering
Bansal institute of science and Technology,
Bhopal (M.P)
baghelerajkumar@gmail.com

Abstract- PVT hybrid systems (photovoltaic and thermal) are solar photovoltaic systems that are combined with a thermal energy system. Because the hybrid system uses the same area to generate both electricity and heat energy, the system's overall efficiency improves Aside from crop drying and air heating, a solar PVT system may be built into a structure's façade, which is known as a building integrated PVT system (BI/PVT). The increasing cost of fossil fuel and crisis of energy has led the world in a quest for exploiting the free and naturally available energy from the sun to produce electric power. This thesis summarizes the development situation of the solar thermal electric technology with description and comparison for three prevalent power generation methods: PV tracking techniques are the methods for positioning solar panels to maximize the quantity of solar irradiation that can be captured. A fixed-tilt solar panel is frequently placed utilizing manually adjustable panel slops, which have the advantages of being cheap cost and simple to install. However, because the sun's location changes during the day or year, they are unable to benefit from the maximum amount of solar irradiation possible PV tracking technology allows a PV array to automatically adapt to the sun's high-density beams. The PV tracker necessitates the purchase of additional components and accessories, such as a motor, gear, control unit, and sensor, which raises the cost of the PV system.

Keywords- PVT, hybrid systems, DG, thermal load, electricity grid.

I. INTRODUCTION

An island is a situation where the power delivery classification is electrically remote from the rest of the electricity system but is still powered by the Directorate-General connected to the grid. Traditionally, there is no active authority cause in the power distribution system, and cannot be obtained power in an upstream transmission line failure event. Still, for DG, this assumption is no longer valid. The recent carry out is that nearly all utilities involve DG to disconnect from network as soon as probable in the island stays.

The IEEE 929-1988 standard [24] involves Directorate-General to be isolated and disconnected. Isolated islands can be intentional or unintentional. During the preservation service of the supply network, the supply network's shutdown may result in generator islands. Since the loss of the network is voluntary, an increase is known. The unintended island phenomenon caused by the unexpected shutdown of the electricity grid has attracted more attention.

There are various problems due to accidental islands. IEEE 1547-2003 standard [25 A delay of up to 2 seconds is required to detect incidental islands and all Directorates-General no longer operate the circulation organization. Traditionally, electricity generation or separation is simply state-owned enterprises. To keep up with increasing demand, various states or counties in North America are deregulating power systems.

This trend is not without the dare. For pattern, how does a dependent power manufacturer (IPP) enter the market? Recent improvements in power electronics technology such as rapid switching, high power insulated bipolar transistors (IGBT), or development of power production technology make DG an essential alternative to alternative communications promote or as additional cogeneration support [8-9].

Although cost per. Kilowatt-hour is still higher than the essential power allotment cost (gas turbine is $ 0.07 / Kw-hr, while the solar power plant is $ 0.5 / KW-hr) [10] [11]. The trend toward complete deregulation of North American power grids or rising fossil fuel costs has led to seeing DG as a viable option. presently, BC Hydro, Canada's third major utility company, has more than 50 dispersed power plants ranging from 0.07 MVA to 34 MVA [12]

This work presents a new method of detection to protect distributed generator feed systems. The technique has been tested on allotment buses of 25 kV or below. The current interest in installing dispersed generators in low-voltage buses near customers has created new security engineers'

disputes, which differ from traditional radial-based security methods. Therefore, it is necessary to reconsider typical protection configurations, such as closed sleepless monitoring, impedance relay security areas, and the discovery of unexpected islands in circulated generator systems. The island situation is defined as when part of the unusable energy production system is isolated from an effective supply system.

It is generally measured undesirable because it can cause potential to injure to existing equipment, cause charge to public utilities, and reduce reliability and power quality. Current island detection methods usually passively and actively monitor over voltage / under voltage and overvoltage / under frequency ratios. However, each technique has ideal sensitive working conditions and insensitive working conditions, and its degree of deterioration in power quality is different, which is called the non-detection zone (NDZ).

The method of recognizing islands proposed in this paper adopts a supposedly precise impedance measurement concept or enlarges it to asymmetrical component impedance sphere using natural and human-made imbalances. In specific applications where this island detection method has improved over the existing island detection method, the general solution has studied where protection engineers can conclude when this technique can efficiently use the majority. First of all, this article first briefly introduces the North American electricity system and the motivation to use distributed production. Then other chapters introduce the background and details of this technology in detail.

II. RELATED WORK

Porta et.al. The study showed that total thermal inertia effect can be fully characterized by a single dimensionless quantity (thermal inertia slenderness ratio). The replications of calibrated mathematical model exemplify effect of thermal inertia on performance. The work on screen distillation, its current status and future prospect s are reviewed and the distillation equipment is classified.

Chouikh et al. The mathematical model of solar peeling plants for desalination of water was used to numerically analyze the natural convection produced by the combined buoyancy effect of thermal diffusion and mass diffusion in the sloping cavity. There is sufficient time for steam cooling A mathematical model of each major component of the solethanol distillation system was established, and the system simulation determined the yield and its concentration under any given condition.

Chang et. al. The solar radiation pattern used for the performance test of thermosyphon solar water heaters was examined and it was concluded that the distribution factor Ri and its standard should be introduced in the CNS test standard to provide reliable test results for the solar water heater .The efficacy of a new type of solar water drying system with a combined heat sink was evaluated, and the theoretical model of the proposed solar collector was compared with the experimental results. The heat efficiency and heat dissipation efficiency of the 12 types of solar thermosyphon water drying systems were modified, and a standard for increasing the efficiency of 0.41 was proposed

III. PROPOSED

A solar thermal power plant is an environmentally friendly way to generate electricity. There are various variables that can impact the quantity of solar radiation available, including daily and seasonal fluctuations in cloud cover, making it difficult to operate a solar thermal power plant efficiently. The majority of renewable energy systems use some sort of solar electricity, whether photovoltaic (PV) or thermal (T). Nonetheless, hybrid solar PV and thermal (PVT) systems remain uncommon.

A single solar panel system or a large-scale solar PV power plant: all of these solar PV systems come in various sizes. Solar thermal systems, on the other hand, are typically seen in individual dwellings and commercial businesses. Temperature, precipitation, air quality, and, most importantly, sun irradiation all influence how effectively solar photovoltaic's function. Solar PV cells, like any other semiconductor device, are temperature sensitive. As the temperature rises, the band gap energy of the semiconductor material decreases, causing the current to rise somewhat but the voltage to fall considerably.

The efficiency of a silicon solar cell reduces by 0.3 percent as the temperature rises by 1°C. If the thermal stress persists, high operating temperatures of solar cells can result in cell efficiency loss and long-term structural damage to the solar panel. This might be up to 50 degrees Celsius greater than the surrounding temperature.

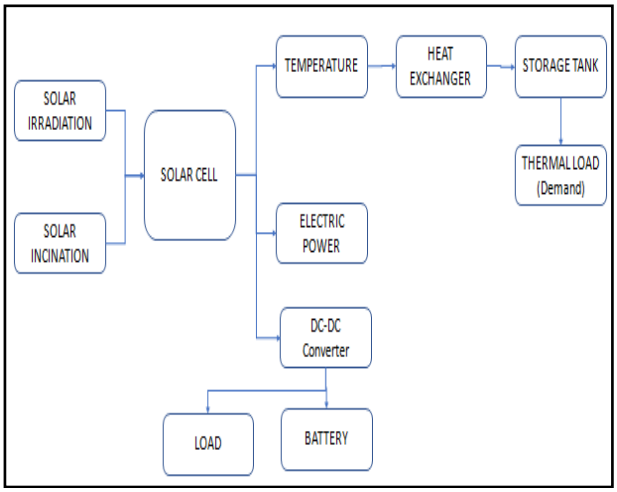

Fig 1. System flow diagram.

PVT hybrid systems (photovoltaic and thermal) are solar photovoltaic systems that are combined with a thermal energy system [4].

Because the hybrid system uses the same area to generate both electricity and heat energy, the system's overall efficiency improves [5]. Aside from crop drying and air heating, a solar PVT system may be built into a structure's façade, which is known as a building integrated PVT system (BI/PVT).

In principle, the overall energy conversion efficiency of a hybrid system may be as high as 60%–80%. Most hybrid systems' electrical performance may be improved by lowering the temperature. [7, 9] Several heat exchangers have been utilized to boost the efficiency of a solar panel by decreasing its temperature.

Table 1. Tank Parameters.

Liquid level	0.9	m
Volume of liquid	tank.Voltank0	m^3
Mass of liquid	5000	kg
Temperature of liquid volume	tank.Ttank0	K
Gravitational acceleration:	9.81	m/s^2

IV. BATTERY

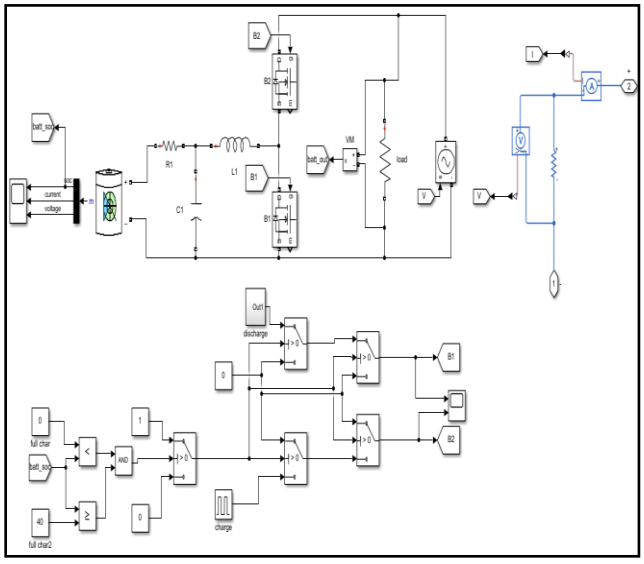

Fig 2. Battery subsystem.

When Fluid inertia is enabled, the liquid will be unable to accelerate as swiftly as previously. It makes use of a generic battery model that is compatible with the great majority of popular battery types.

The effects of lithium-ion battery type, temperature, and age (due to cycling) may be noted.

V. SIMULATION RESULTS

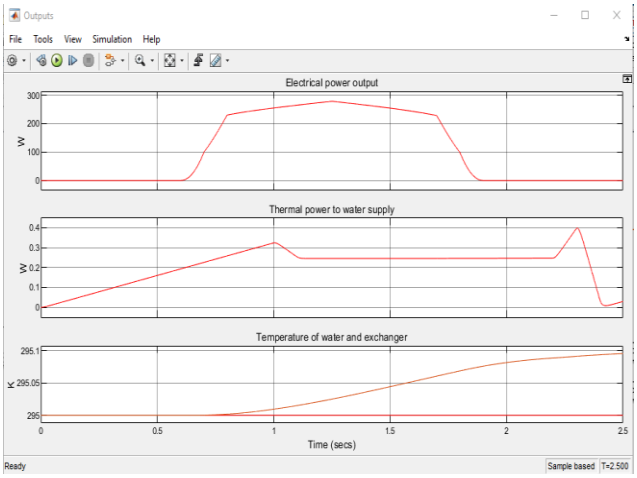

Fig 3. Electrical power output, thermal power to water supply, tempreture of water and exchanger.

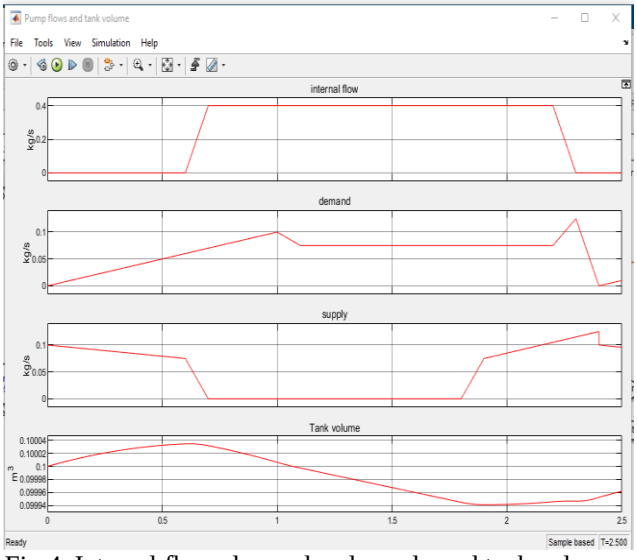

Fig 4. Internal flow, demand and supply and tank volume.

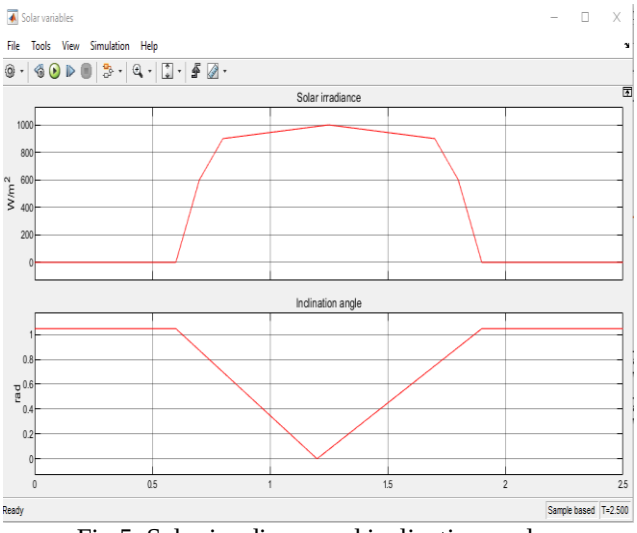

Fig 5. Solar irradiance and inclination angle.

Table 2. Simulation Output Value.

Parameter	Output
Electrical power output	275.1
Thermal power to water supply	250 w
Temperature of water and exchanger	0.33 w

VI. DEVELOPMENT OF A MODEL OF THE TECHNICAL AND ECONOMIC CHARACTERISTICS OF THE HYBRID POWER PLANT

Topology and Design Principle of Grid-Connected PV and thermal energy Hybrid System This section discusses the system's design and operational principles, with Figure 1 depicting a schematic illustration of the system. The first part of the system is a hybrid power system that comprises PV and thermal energy, while the second is grid-dependent. The dispatch energy management and thermal energy are important components of the hybrid power system. PV modules and are also part of the system. The actual load data, solar radiation, and ambient temperature are all considered.

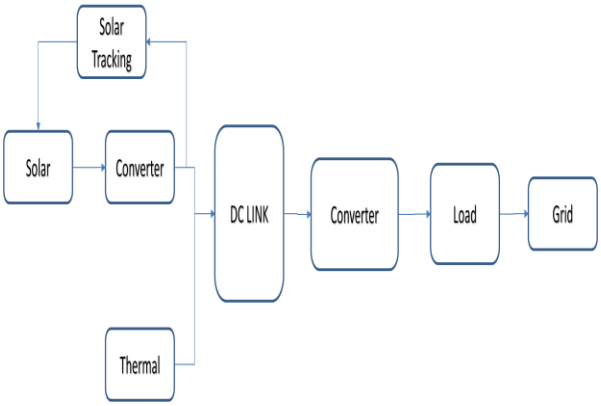

Fig 6. System block of hybrid energy power plant.

VII. THE DESIGN OF HYBRID SYSTEM COMPONENTS

1. Solar PV Models:
The DC bus bar was supplied with DC electricity from the PV technology using solar power. System constraints, such as the minimum proportion of renewable energy considered, the maximum capacity of the grid sold back, the density of solar irradiation, and the load necessary, defines the scale of the PV model. The PV models should have enough capacity for peak load as well as additional power for the hybrid system, which can be sold back to the grid.

2. PV Tracking Techniques:
PV tracking techniques are the methods for positioning solar panels to maximize the quantity of solar irradiation that can be captured. A fixed-tilt solar panel is frequently placed utilizing manually adjustable panel slops, which have the advantages of being cheap cost and simple to install. However, because the sun's location changes during the day or year, they are unable to benefit from the maximum amount of solar irradiation possible [14].

PV tracking technology allows a PV array to automatically adapt to the sun's high-density beams. The PV tracker necessitates the purchase of additional components and accessories, such as a motor, gear, control unit, and sensor, which raises the cost of the PV system [57].

The four most often utilized PV tracking methods in this study are:

- **Fixed-tilt solar panel (FTSP):** The solar arrays azimuth and tilt are both fixed. This is the most common and simple way.
- **Horizontal single-axis tracker (HSAT):** The PV array is horizontal in orientation (east-west). While the azimuth stays constant, the tilt angle fluctuates in response to the angle of incidence.
- **Vertical single-axis tracker (VSAT):** The photovoltaic array is oriented north-south. To match the angle of incidence, the azimuth and tilt angle are both changed at the same time.
- **Dual-axis tracker (DAT):** Because of the manner it was constructed, the solar array can rotate both horizontally and vertically. Because the surfaces of the panels are perpendicular, the incidence angle is always perpendicular to them.

Table 2.54 demonstrates the economic costs of horizontal, vertical, and dual-axis trackers, and Figure 2.54 depicts the four PV tracking systems [56].

Table 3. The economic cost of different PV tracking techniques.

PV Tracking System	$/kWh
Horizontal single axis tracker (HSAT)	880
Vertical single axis tracker (VSAT)	265
Dual axis tracker (DAT)	1000

3. Electrolyzer:
Water is electrolyzed in an electrolyzer, which is a device that divides water into hydrogen and oxygen using electricity. There is an abundance of renewable energy sources that might be utilized in the electrolysis process. Gases are released based on electrolyzer capacity and current flow via its cells [66]. Alkaline electrolysis was chosen for this method due to its wide use and low cost when compared to other electrolyzer technologies. [67]

4. Hydrogen Tank:
The hydrogen produced by the electrolyzer must be stored in a tank before it can be used by the FC. The tank has a capacity of 0–1200 kg and a life expectancy in the search

space of 25 years. The economic tank parameters for capital, replacement, and O&M expenses are 1400 $/kg, 867 $/kg, and 20 $/year, respectively [42].

5. Grid:
This implies that when demand exceeds the amount of power purchased by the grid, FC is used to replenish the grid's supply of electricity. During the day, excess solar electricity is provided to the load, while the balance is sold back to the utility grid.

6. Feed-in tariff (REFIT):
A strategic agreement with renewable energy sources to sell back to the grid at a reduced cost. The parameters of this agreement differ from country to country in order to enhance the penetration of renewable energy.

6. Energy Dispatch Principle of the Hybrid System:
A load following approach is used to send energy. The fuel cell is only triggered in this manner when PV and the grid are unable to meet demand. The backup power of the fuel cell cannot be used to power the electrolyzer. The feed electrolyzer is powered by excess PV electricity. Furthermore, when the demand for hydrogen creation exceeds the capacity of the PV system, the PV electricity generated will be sold to the grid. Because of the smaller generator size, dispatched energy is frequently used for the following load. [72].

A hybrid renewable energy/distributed generation (DG) system that employs a smaller generator to meet important demands but not for additional tasks like providing batteries or an electrolyzer has environmental benefits. [73].

VIII. RESULTS AND DISCUSSION

Based on modeling results, the grid-connected hybrid energy system may be implemented in a number of ways (PV-FC). Four of the most important PV tracking approaches researched to establish the system's best techno-economic characteristics are FTSP, HSAT, VSAT, and DAT. Furthermore, the optimal design's operating statuary with the best PV monitoring technology selection is illustrated. The results are presented in three sections here.

1. Comparison of Various PV Tracking Techniques on the Technical Aspect:
The technological components of the grid-connected hybrid system received a lot of interest (PVT). PV production is presented in 2.55 on a yearly basis. When it comes to generating high PV power generation, both VSAT and FTSP are obviously in the lead. VSAT, on the other hand, performs significantly better between April and August. With the exception of the months of April–August, DAT is more suited to high-power outputs than HSAT.

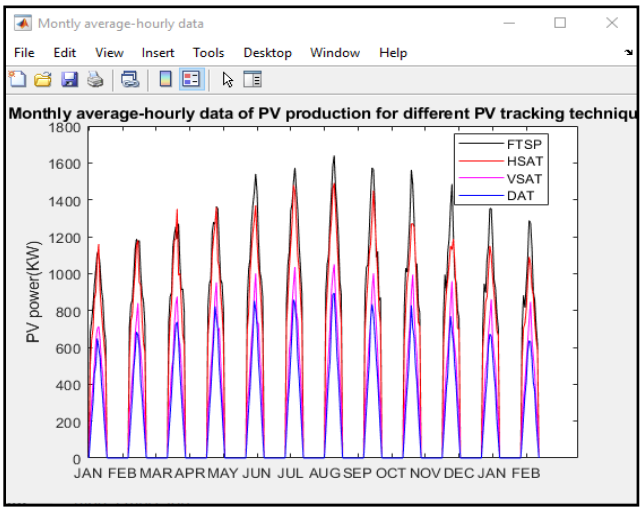

Fig 7. Monthly average-hourly data of PV production for different PV tracking techniques.

According to Figure 11a, the FTSP, HSAT ,VSAT, DAT, and create the Monthly average-hourly data of PV production for different PV tracking, followed by 1639 MWh/year, followed by 1500MWh/year, 1029 MWh/year, and 888 MWh/year, respectively.

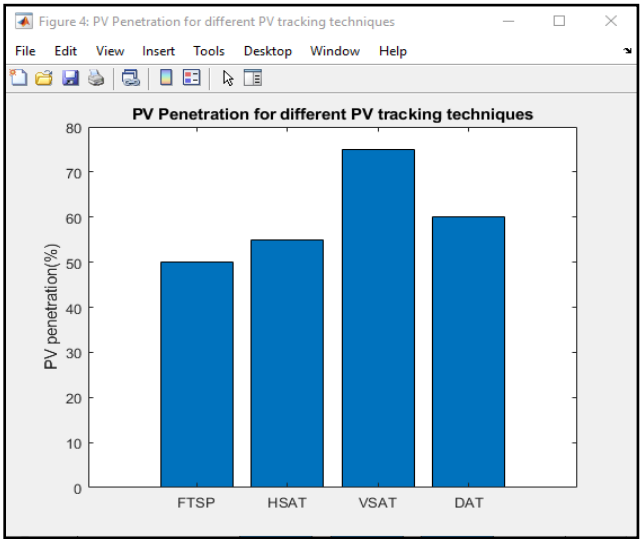

Fig 8. PV penetration for different PV tracking techniques.

When addressing this, it is critical to consider PV penetration. In the grid-connected hybrid system (PV/FC) HSAT had the greatest PV penetration of 75 percent, followed by FTSP,VSAT, DAT at 55 percent, and 75 percent and 60% respectively. As a result, there is a 20 percent difference between the greatest and lowest values between the FTSP, and the VSAT,

According to Figure4.22, the FTSP, HSAT, VSAT, DAT create the greatest yearly PV power, with 9032.0 MWh/year, followed by 7395.0 MWh/year, 1388.0 MWh/year, and 9051.0 MWh/year, respectively. In terms of power generation, the DAT generated more electricity

than the FTSP, DAT, and HSAT.In terms of power generation.

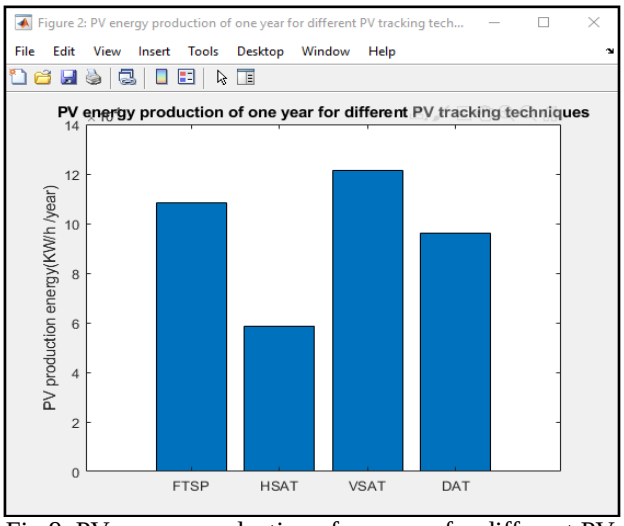

Fig 9. PV energy production of one year for different PV tracking techniques.

In terms of power generation, the FTSP generated 50 percent, 55 percent, and 75 percent and 60% more electricity than the FTSP, DAT, and HSAT. The VSAT generated 60% percent more electricity than the FTSP, DAT, and HSAT

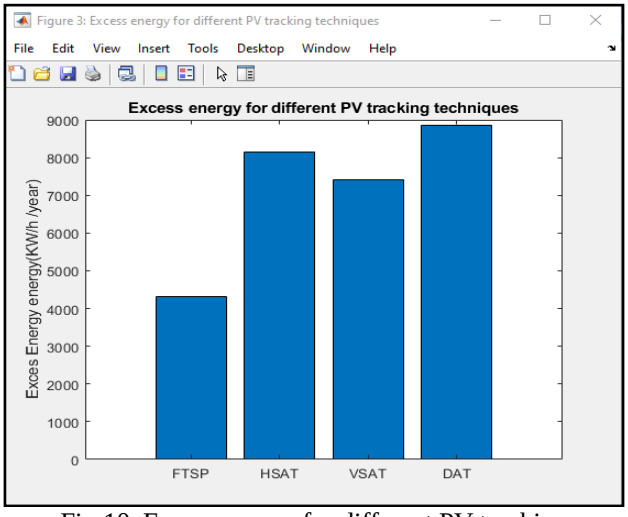

Fig 10. Excess energy for different PV tracking techniques.

The excess electricity in the system was caused by the PV system's output surpassing the system's use. Surplus electricity in a Microgrid hybrid renewable power system is generally dumped or can be used for other reasons. According to a new study, the excess power generated will be reinvested in the system, bringing in additional money.

As indicated in Figure 4.23 FTSP, DAT, and HSAT. The VSAT are listed sequentially next in this model, with a total surplus energy of 3690 MWh/year, followed by 11520 MWh/year, 6350 MWh/year, and 8925 MWh/year, respectively.

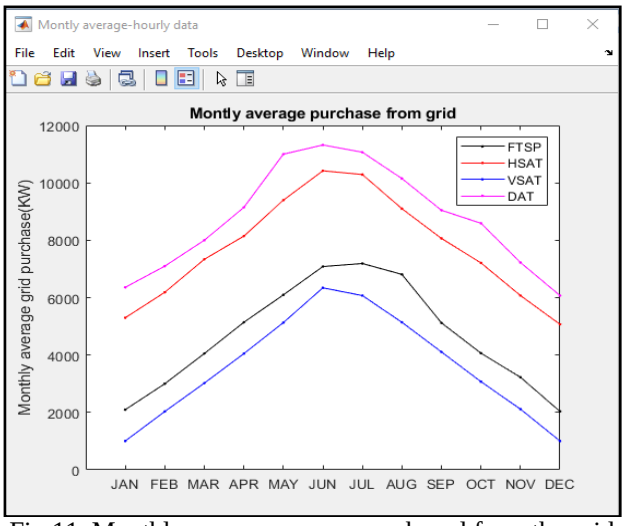

Fig 11. Monthly average energy purchased from the grid for different PV tracking techniques.

Taking four PV monitoring methodologies, each month's energy purchases and sales may be explored in greater depth. The curves in Figure 4.24, which illustrates the monthly average amount of power, purchased from a utility, show that DAT, HSAT, FTSP, and VSAT all had the highest energy purchases for the calendar year.

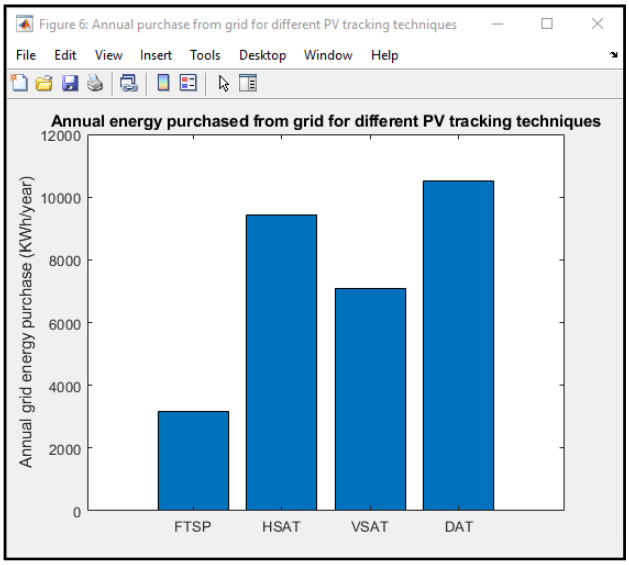

Fig 12. Energy acquired from the grid on a yearly basis for various PV tracking approaches.

The greatest quantity of energy is purchased during the summer months. Figure 4.25 illustrates the yearly total energy expenditures in a simple and easy-to-understand manner. In terms of yearly ,The chart depicts the FTSP's, estimated annual energy usage of 3000 MWh/year, followed by HSAT's 1056.0 MWh/year, VSAT's 5250.0 MWh/year, and DAT's 8550.0 MWh/year.

International Journal of Scientific Research & Engineering Trends
Volume 8, Issue 2, Mar-Apr-2022, ISSN (Online): 2395-566X

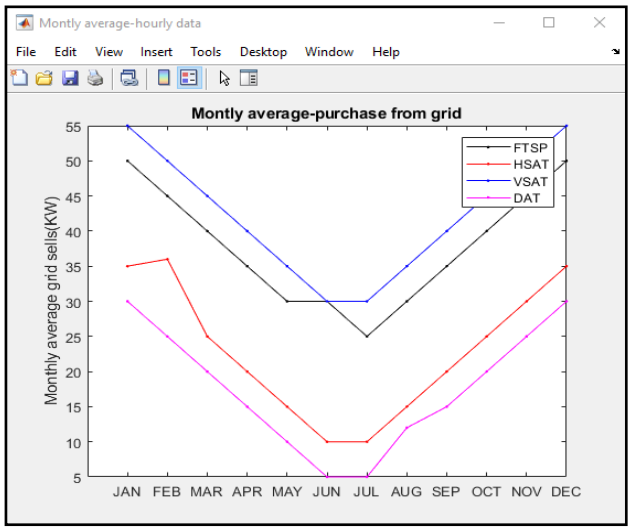

Fig 13. Monthly average energy sold to the grid for different PV tracking techniques.

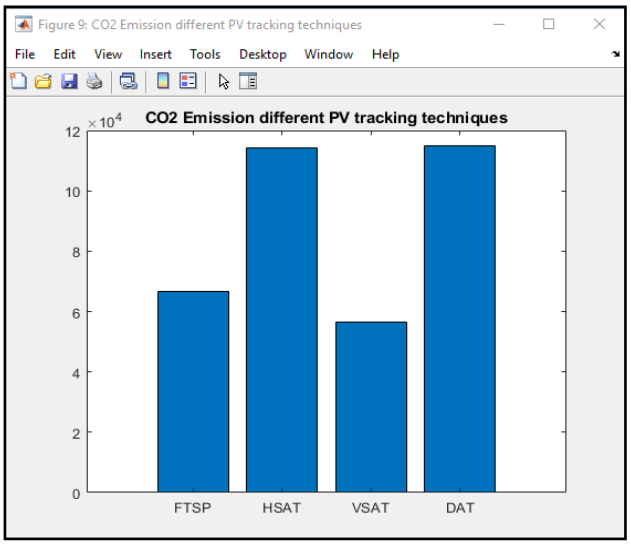

Fig 14. CO2 emissions for different PV tracking techniques.

This is depicted in Figure 4.26, which illustrates the monthly average of grid sales for each month. According to the statistics, VSAT has the highest monthly average energy sold back to the grid. Aside from the fact that HSAT and DAT sold the least quantity of energy, there was no difference in yearly total sold energy.

It was also discovered that the summer months had the lowest energy sales because demand for load energy was at its peak, taking four PV monitoring methodologies, each month's energy purchases and sales may be explored in greater depth. The curves in which illustrates the monthly average amount of power purchased from a utility, show that FTSP, DAT, and HSAT. The VSAT and DAT all had the highest energy purchases for the calendar year.

In order to create electricity in Iraq, a significant amount of fossil fuel is necessary. In other words, CO2 emissions were directly related to oil projections. With Iraqi oil output surpassing (4.78 million barrels per day) in 2018, CO2 emissions reached a new high of 188.1 million tones. CO2 emissions increased by 2% over the study period (65.176 percent). CO2 emissions were shown to be inversely associated to CI.

According to Figure 4.25 the lowest CO2 emissions were achieved by DAT, which generated a total of 1125.0 kilogram's per year, followed by FTSP, HSAT, and DAT, each of which produced a total of 57100.0 kilogram's per year,HSAT has 8880.0 kilogram's per year and VSAT has 4896.0 kilograms per year. Illustrate how VSAT technology assists in purchasing the least amount of energy from the grid while selling the most. Grid-connected hybrid energy systems (PVFCs) may be developed utilizing four different PV tracking approaches, however the vertical single axis tracker (VSAT) is the best choice at the location of this investigation.

2. Comparison of Various PV Tracking Techniques on the Economic Aspect:

Criteria for Economic Analysis the economic comparison of several proposed designs is based on NPC and LCOE. Homer is used to compute the NPC, which is the current cost minus salvage and money earned by selling electricity to the grid. The current cost in this case includes the capital cost, replacement cost, and O and M of the entire system across the project life cycle. The salvage is the worth of the leftover components at the conclusion of the investment. Equation (2) [69] may be used to calculate it.

$$\mathbf{NPC} = \frac{C_{ann,tot}}{CRF(i,N)}$$

Total annual cost of the system in dollars (Cann,tot) Capital recovery is abbreviated as CRF. The life cycle of the project is N. The yearly real interest rate is I according to the formula [34].

$$\mathbf{I} = \frac{i^{0}-f}{1-f}$$

Where I o denotes the nominal interest rate, or the rate at which you may borrow money (percent). f is the annual inflation rate, which is the predicted inflation rate during the project's lifetime in dollars (percent).
[69] provides a formula for calculating the capital recovery factor.

$$\mathbf{CRF(i, N)} = \frac{i(1+i)^{N}}{(1+i)^{N}-1}$$

The average cost of energy unit is the levelized cost of energy (LCOE) (kWh). Homer can figure it out by dividing the total yearly cost of the complete system with the total energy generated in one year. Equation [14] may be used to represent it as follows:

$$\mathbf{LCOE}\left(\frac{(\$)}{kWh}\right) = \frac{C_{ann,tot}}{R_{prim}+R_{tot,grid,sales}}$$

Rprim is the main served load in kWh/year, and Rtot, grid.sales is the total grid sold electricity in kWh/year. All types of expenses were included in the yearly total cost, including annualized capital, replacement, and O and M costs.

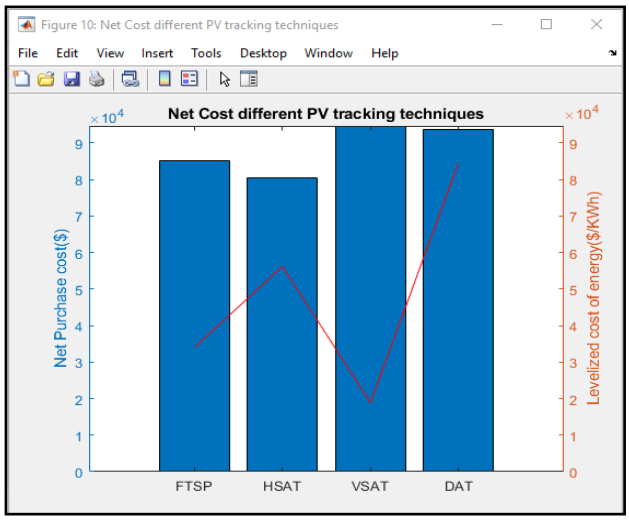

Fig 15. Net cost for different PV techniques.

Four alternative grid-connected hybrid energy systems (PVT) were compared to demonstrate a wide variety of PV tracking options. Figure 4.28 shows that VSAT technology has the lowest NPC and LCOE, which are 3760.00$/kWh and 6866.0$/kWh, 1554.0 $/kWh, 1020.0 $/kWh respectively.

The HSAT generated 6866.0$/kWh and 0.2739$/kWh, ranking second in terms of NPC and third in terms of LCOE. In terms of net present value (NPV) and net present value per kWh, the VSAT ranks third in terms of NPC and second in terms of net present value per kWh (NPV). In compared to the highest NPC, LOCE, which received 3990264$ and 0.2878$/kWh, HSAT ranks last.

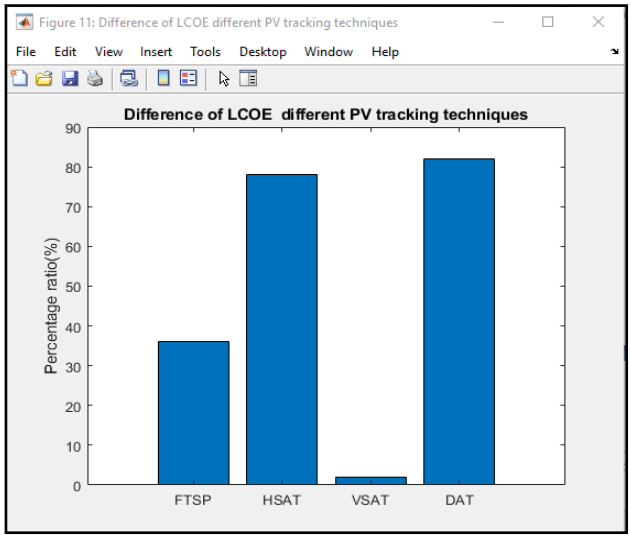

Fig 16. Different of LCOE for different PV techniques.

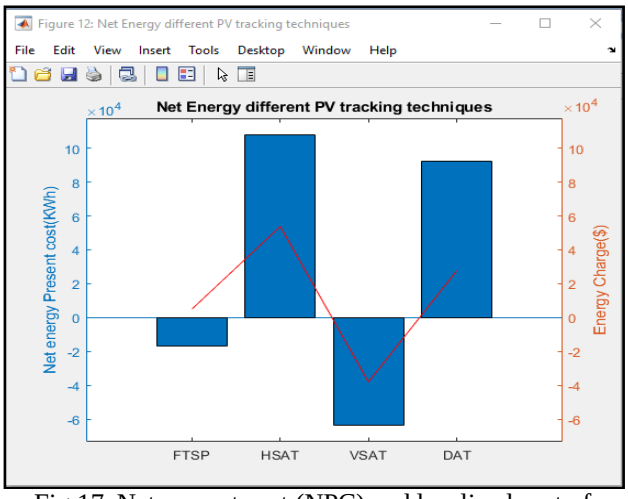

Fig 17. Net present cost (NPC) and levelized cost of energy (LCOE) for different PV tracking techniques.

Figure 4.30 shows how the LCOEs of various PV trackers were compared to the basic case of VSAT, which had the lowest LCOE. In terms of LCOE, VSAT was determined to be 37.65 percent less expensive than FSAT, HDAT, and DAT. energy is defined as the quantity of power purchased minus the amount of electricity sold early. In other words, if the net purchased energy is negative, it means that the sold energy exceeded the purchased energy, or vice versa. As a result, a negative energy charge shows that the expenses of selling power are more than the costs of obtaining electricity.

Estimates of net purchased energy for several PV tracking devices demonstrate which PV tracker earned the greatest money, lowering the LCOE. VSAT technology had the greatest net purchased energy, indicates that, as predicted, the grid-based technique is more reliable for DAT than it is for HSAT. The LCOE has risen somewhat as a result of the system's modest contribution of renewable energy, as previously stated. However, with VSAT and FTSP, the design system sold more energy than was purchased.

These two designs contributed more to renewable energy generation, resulting in a reduced LCOE for the system. A vertical single axis tracker (VSAT) provides increased economic feasibility for the proposed grid-connected hybrid energy system (PV-FC) based on meteorological data and the unique location.

IX. CONCLUSION

In the next section study investigated the effects of the primary four PV tracking methodologies on the technical and economic performance of a grid-connected hybrid power system (PVT). FTSP, HSAT, VSAT, and DAT were among the most significant PV tracking systems investigated. The findings were simulated, calculated, and optimized using the MATLAB programme. Furthermore, the system's component makers submitted technical and

economic data. PV tracking techniques were tested for their influence on the techno-economic performance of the proposed system, and the results were carefully discussed and contrasted. According to the findings, VSAT was shown to be the most efficient in terms of yearly energy output, followed by FTSP, DAT, and HSAT, in that order.PV penetration data reveal that VSAT had a 772 percent larger PV penetration of solar energy to the grid than DAT (674 percent), HSAT (595 percent), or FTSP (563 percent VSAT sold the more energy to the grid than the others in terms of net bought energy.

Using the VSAT as the base case with the lowest LCOE, the VSAT may reduce the LCOE by 37.65%, 77.5 percent, and 86.5 percent, respectively, when compared to the FTSP, HSAT, and DAT.VSAT emissions were determined to be the least damaging, whereas DAT emissions were shown to be the most detrimental. As a result, it grew more reliant on the grid. In this situation, VSAT has the lowest environmental effect. The study discovered that VSAT plays a critical role in optimizing technical performance and lowering the proposed system's economic cost.

As a result, VSAT is a strong contender for the finest grid-connected hybrid (PV-FC) energy system The suggested system design approach and PV tracker inquiry have been validated for every place on the planet, albeit the outcome may vary depending on component pricing and metrological data.In the next section advance prototype test designed in the detailed the mathematical model and representation of the system under design, The considered FPC (Flat Plate Collector)comprises an absorber, annulus, cover, and tubes while the model accounts for the dynamic thermal responses of the absorber, cover, and working fluid

REFERENCES

[1] E. Carroll, High power active devices, CAS Power Converters for Particle Accelerators, Warrington, 2004.
[2] Rufer, Passive components, CAS Power Converters for Particle Accelerators, Warrington, 2004.
[3] H. Foch and J. Roux, Convertisseurs statiques d'énergie électrique à semi-conducteurs, Patent FR 78324428, US patent 093106 (1978).
[4] H. Foch, P. Marty and J. Roux, Use of duality rules in the conception of transistorized converters, PCI Proceedings, Munich, 1980.
[5] Y. Cheron, H. Foch and T. Meynard, Generalization of the resonant switch concept: Structures and performance, Power Electronics and Applications, EPE, Grenoble, September 1987.
[6] Y. Cheron, Soft Commutation (Chapman & Hall, 1992) (ISBN 0 412 39510 X).
[7] R. Arches, F. Bordry, Y. Cheron, B. Escaut, H. Foch, P. Marty and M. Metz, Principe's fondamentaux: Commutation dans les convertisseurs statiques, in D 3153, Techniques de l'Ingénieur, Traité de Genie Electrique, 9-1989.
[8] F.C. Lee, Zero-voltage switching techniques in DC-DC converter circuits, High Frequency Power Conversion Conference, Washington, April 1998.
[9] Bordry, Power converters for particle accelerators: development and production of the Large Hadron Collider (LHC) powering system, PCIM Conference, Nürnberg, Germany, 7-9 June 2005.
[10] Bordry, G. Kniegl, V. Montabonnet, R. Pauls, H. Thiesen and B. Wolfes, Soft-switching (ZVZCS) high-current, low voltage modular power converter, 9th European Conference on Power Electronics EPE2001, Graz, Austria, September 2001.
[11] Bordry, V. Montabonnet, D. Nisbet, P. Korhonen, R. Turunen and H. Volotinen, Development, test and large production of soft-switching high current power converters for particle accelerators, 11th European Conference on Power Electronics EPE2005, Dresden, Germany, September 2005.
[12] H. Foch, P. Marty and Y. Cheron, DC and slow pulsed converter topologies, CAS Power Converters for Particle Accelerators, Montreux, 1990, CERN 90-07.
[13] R. Arches, F. Bordry, Y. Cheron, B. Escaut, H. Foch, P. Marty and M. Metz, Principes fondamentaux: Eléments constitutifs et synthèse des convertisseurs statiques, in D 3152, Techniques de l'Ingénieur, Traité de Genie Electrique, 6-1989.
[14] E. Carroll, High power active devices, CAS Power Converters for Particle Accelerators, Warrington, 2004.
[15] Rufer, Passive components, CAS Power Converters for Particle Accelerators, Warrington, 2004.
[16] Foch and J. Roux, Convertisseurs statiques d'énergie électrique à semi-conducteurs, Patent FR 78324428, US patent 093106 (1978).
[17] H. Foch, P. Marty and J. Roux, Use of duality rules in the conception of transistorized converters, PCI Proceedings, Munich, 1980.
[18] Cheron, H. Foch and T. Meynard, Generalization of the resonant switch concept: Structures and performance, Power Electronics and Applications, EPE, Grenoble, September 1987.
[19] Cheron, Soft Commutation (Chapman & Hall, 1992) (ISBN 0 412 39510 X).
[20] R. Arches, F. Bordry, Y. Cheron, B. Escaut, H. Foch, P. Marty and M. Metz, Principes fondamentaux: Commutation dans les convertisseurs statiques, in D 3153, Techniques de l'Ingénieur, Traité de Genie Electrique, 9-1989.
[21] F.C. Lee, Zero-voltage switching techniques in DC-DC converter circuits, High Frequency Power Conversion Conference, Washington, April 1998.